

ALMA observations of super-early galaxies: attenuation-free model predictions

A. FERRARA ¹, S. CARNIANI ¹, F. DI MASCIA ¹, R.J. BOUWENS ², P. OESCH ^{3,4} AND S. SCHOUWS ²

¹*Scuola Normale Superiore, Piazza dei Cavalieri 7, 50126 Pisa, Italy*

²*Leiden Observatory, Leiden University, NL-2300 RA Leiden, Netherlands*

³*Observatoire de Genève, 1290 Versoix, Switzerland*

⁴*Cosmic Dawn Center (DAWN), Niels Bohr Institute, University of Copenhagen, Jagtvej 128, København N, DK-2200, Denmark*

(Revised September 27, 2024)

ABSTRACT

The abundance and blue color of super-early (redshift $z > 10$), luminous galaxies discovered by JWST can be explained if radiation-driven outflows have ejected their dust on kpc-scales. To test this hypothesis, we predict the ALMA detectability of such extended dust component. Given the observed properties of the galaxy, its observed continuum flux at 88 μm , F_{88} , depends on the dust-to-stellar mass ratio, ξ_d , and extent of the dust distribution, r_d . Once applied to the most distant galaxy known, GS-z14-0 at $z = 14.32$, the fiducial model ($\xi_d = 1/529$) predicts $F_{88}^{\text{fid}} = 14.9 \mu\text{Jy}$, and a dust extent $r_d = 1.4$ kpc. If the galaxy is very dust-rich ($\xi_d = 1/40$), $F_{88}^{\text{max}} = 40.1 \mu\text{Jy}$. These values are smaller ($F_{88}^{\text{fid}} = 9.5 \mu\text{Jy}$) if the dust is predominantly made of large grains as those formed in SN ejecta. Forthcoming ALMA observations might come very close to constraining the fiducial predictions of the outflow-based attenuation-free model. Other super-early galaxies are predicted to be fainter at 88 μm , mostly because of their lower SFR compared to GS-z14-0, with fiducial fluxes in the range 2 – 5.2 μJy .

Keywords: galaxies: high-redshift, galaxies: evolution, galaxies: formation

1. INTRODUCTION

The approximately fifteen galaxies discovered so far by the *James Webb Space Telescope* (JWST) at redshift $z > 10$ (Naidu et al. 2022; Arrabal Haro et al. 2023; Hsiao et al. 2023; Wang et al. 2023; Fujimoto et al. 2023a; Atek et al. 2022; Curtis-Lake et al. 2023; Robertson et al. 2023a; Bunker et al. 2023; Tacchella et al. 2023; Arrabal Haro et al. 2023; Finkelstein et al. 2023; Castellano et al. 2024; Zavala et al. 2024; Helton et al. 2024; Carniani et al. 2024; Robertson et al. 2023b) have raised a number of questions concerning early galaxy evolution. Not only their number significantly overshoots extrapolations and models anchored at lower redshifts, but these objects also share some peculiar properties whose origin

constitute a challenging puzzle for Λ CDM-based¹ galaxy formation scenarios.

At odd with their lower redshift counterparts, many super-early galaxies are characterised by bright UV luminosities ($M_{\text{UV}} \lesssim -20$), steep UV spectral slopes ($\beta \lesssim -2.2$), compact sizes (effective radius $r_e \approx 200$ pc). The analysis of their Spectral Energy Distribution suggests large (for their epoch) stellar masses ($M_\star \approx 10^9 M_\odot$), thus identifying these rare systems as high- σ peaks of the cosmic density field populating the bright-end of the luminosity function. Several alternative hy-

¹ Throughout the paper, we assume a flat Universe with the following cosmological parameters: $\Omega_M = 0.3075$, $\Omega_\Lambda = 1 - \Omega_M$, and $\Omega_b = 0.0486$, $h = 0.6774$, $\sigma_8 = 0.826$, where Ω_M , Ω_Λ , and Ω_b are the total matter, vacuum, and baryon densities, in units of the critical density; h is the Hubble constant in units of 100 km s^{-1} , and σ_8 is the late-time fluctuation amplitude parameter (Planck Collaboration et al. 2014).

potheses have been suggested to explain the above properties².

According to the so-called ‘‘Attenuation-Free Model’’ (AFM, Ferrara et al. 2023; Ziparo et al. 2023; Fiore et al. 2023; Ferrara 2024a,b) bright luminosities and blue colors result from extremely low dust attenuation conditions. These could be due to low absorbing dust column density, or to grain optical properties producing ‘‘gray’’, relatively transparent extinction curves (see, e.g. Markov et al. 2024) at high redshift.

AFM postulates that dust has been produced in supernova (SN) ejecta with standard net³ yields $y_d \approx 0.1M_\odot/\text{SN}$. After their injection into the interstellar medium, grains could either grow by gas-phase heavy elements accretion and/or be partially destroyed by shocks. However, at $z > 10$ the prevailing physical conditions result in timescales of both processes are longer than the Hubble time, thus making them ineffective (Ferrara et al. 2016; Hirashita & Aoyama 2019; Martnez-Gonzalez et al. 2019; Lesniewska & Michaowski 2019; Dayal et al. 2022; Priestley et al. 2021). The same argument applies to other known dust sources, such as AGB and evolved stars (Ferrarotti & Gail 2006; Valiante et al. 2009).

Corroborated by the evidence for significant amounts of heavy elements in many super-early galaxies (Curti et al. 2022; Bunker et al. 2023; Calabro et al. 2024), it is physically sound to assume that dust was also copiously produced by the large number ($\approx 10^7$) of SNe in these galaxies. Moreover, due to their very compact size, Ferrara (2024a) have shown that in a few Myr the produced dust would completely obscure the galaxy. Instead, *JWST* spectra indicate extremely small V-band attenuations, $A_V \lesssim 0.3$.

To unify several aspects of the problem, it has been proposed that, in spite of the large stellar masses, attenuation-free conditions can be established by outflows (Ziparo et al. 2023; Fiore et al. 2023). As these objects have most often luminosities exceeding the effective Eddington luminosity for a dusty medium (Ferrara 2024a), which can be to first order translated in a lower bound on the specific star formation rate

$\text{sSFR} > 25 \text{ Gyr}^{-1}$, they can launch powerful outflows driven by radiation pressure on the dust itself.

As $A_V \propto r_d^{-2}$, where r_d is the radial extent of the dust distribution, the outflow can effectively reduce the attenuation by transporting dust on larger spatial scales. For example, expanding the distribution from $r_e \approx 200$ pc to ≈ 2 kpc, would cause a dramatic drop of the UV optical depth by 100 times, making the galaxy almost transparent and bright. Thus, AFM predicts that dust should be significantly more extended than the stars in super-early galaxies. Moreover, such dust component should emit thermal far infrared (FIR) continuum due to grain reprocessing of the absorbed UV/optical light from the stars within r_e .

Here we aim at assessing whether the FIR signal produced by such extended dust distribution produced by outflows can be detected by the *Atacama Large Millimeter Array* (ALMA). The detection depends on several factors, such as the dust (i) spatial extent, (ii) mass, and (iii) temperature (including CMB effects), and (iv) grain optical properties. This experiment represents a stringent test for the AFM.

In this Letter, we mainly concentrate on the specific, but yet utmost important, case of the most distant galaxy known, GS-z14-0 ($z = 14.32$, Carniani et al. 2024) for which the required ALMA data will become soon available (DDT 2023.A.00037.S, PI: S. Schouws).

A positive detection would strongly support the idea that dust is produced by SNe, and subsequently ejected by outflows outside the galaxy main body. A non detection would instead put meaningful upper limits on early dust production and properties at these yet basically unexplored cosmic epochs. We also apply the model to four additional $z > 10$ galaxies.

2. FIR DUST CONTINUUM EMISSION

To predict the expected FIR continuum emission, we first quantify the dust production and its spatial distribution. Next, we compute the dust temperature including CMB and radiative transfer effects. From these quantities we finally obtain the observed FIR flux from a given galaxy.

2.1. Dust production

At high redshift ($z > 7$) dust production can be safely assumed to be largely dominated by SNe (Todini & Ferrara 2001; Lesniewska & Michaowski 2019; Dayal et al. 2022; Sommovigo et al. 2022; Ferrara et al. 2022; Schneider & Maiolino 2024) as grain growth (Ferrara et al. 2016; Hirashita & Aoyama 2019) is sub-dominant, and other known sources (AGB and evolved stars, Valiante et al. 2009) have evolutionary times exceeding the Hubble time (294 Myr at $z = 14.32$).

² These include (a) star formation variability (Mason et al. 2023; Mirocha & Furlanetto 2023; Pallottini & Ferrara 2023), (b) reduced feedback resulting in a higher star formation efficiency (Dekel et al. 2023; Li et al. 2023), and (c) a top-heavy IMF (Inayoshi et al. 2022), although see Rasmussen Cueto et al. (2023). More exotic solutions involving primordial black holes have also been suggested (Liu & Bromm 2022).

³ That is, after reprocessing by the reverse shock thermalizing the ejecta

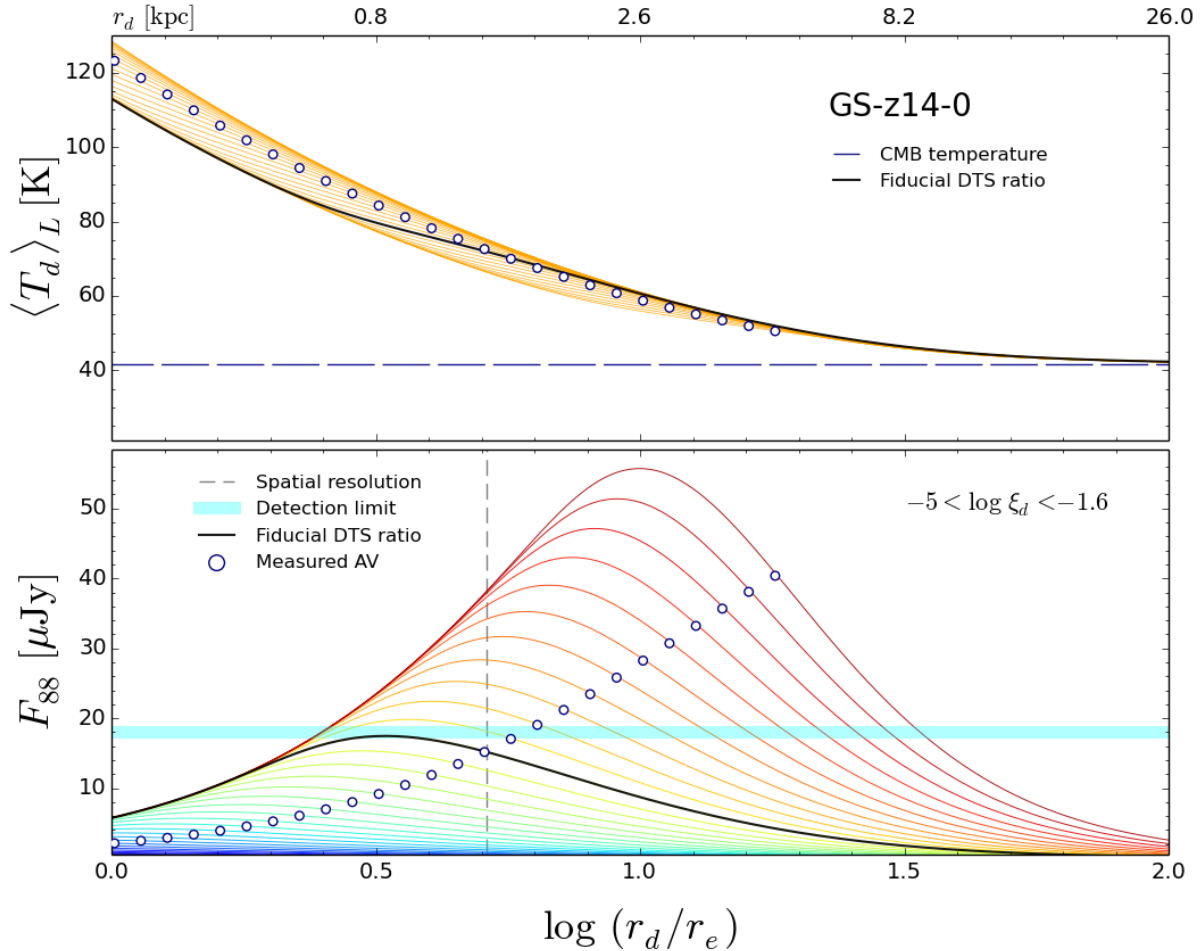


Figure 1. *Top panel:* Temperature distribution as a function of the dust spatial distribution radius, r_d , in units of the effective stellar radius of GS-z14-0, $r_e = 260$ pc. The different orange curves span the dust-to-stellar ratio range $-5 < \log \xi_d < -1.6$ equally spaced in 0.1 logarithmic intervals, with the black curve highlighting the fiducial case $\log \xi_d = -2.72$ ($\xi_d = 1/529$). Also shown is the CMB temperature at the galaxy redshift $z = 14.32$. The circles indicate the radius for which A_V of the galaxy matches the observed one, $A_V = 0.31$. *Bottom panel:* As in the top panel, but for the predicted observed flux from GS-z14-0 at 88μ . Also shown are the expected 3σ sensitivity limit ($18\mu\text{Jy}/\text{beam}$), and spatial resolution ($0.418''$) of the DDT 2023.A.00037.S (PI: S. Schouws) observations.

We assume that stars form according to a Salpeter Initial Mass Function in the range $1 - 100 M_\odot$. As a result, a SN occurs every $\nu^{-1} = 52.9 M_\odot$ of stars formed.

The dust yield per SN is rather uncertain as it involves complex nucleation physics of heavy elements in the SN ejecta. Also, newly formed grains are subject to destruction processes when they pass through the reverse shock. The net production yield is therefore poorly constrained, but based also on local SN studies (Matsuura et al. 2015; Rho et al. 2018; Priestley et al. 2021; Niculescu-Duvaz et al. 2021), it ranges from 0.01 to $1.1 M_\odot$. Therefore we use $y_d = 0.1 M_\odot$ as a fiducial value.

Given the IMF, this corresponds to a dust-to-stellar ratio $\xi_d = y_d \nu = 1/529$. However, given the above un-

certainities, we explore the implications of the wide range of values $-5 < \log \xi_d < -1.6$. This range should therefore encompass both a situation in which freshly formed dust is heavily destroyed by the reverse shock, and a super-efficient dust condensation under very favourable conditions.

For the fiducial value of ξ_d and the measured stellar mass of GS-z14-0 ($M_\star = 4 \times 10^8 M_\odot$; Carniani et al. 2024), we find that $7.5 \times 10^5 M_\odot$ of dust should have been produced by the time of the observation. We recall that dust typically condenses in the ejecta few hundreds of days after the explosion (Todini & Ferrara 2001; Nozawa et al. 2007). For our purposes dust production can be considered as instantaneous, and occurring on the same

evolutionary timescale of SN massive star progenitors, i.e., $\lesssim 20$ Myr.

2.2. Dust spatial distribution

Initially, the dust is distributed as the observed massive stars providing the observed rest frame UV luminosity. In GS-z14-0, these are distributed within a measured effective radius $r_e = 260$ pc. Under this hypothesis, the dust optical depth at 1500 \AA would be equal to $\tau_{1500}^e = (\kappa_{1500} \xi_d / 4\pi r_e^2) M_\star = 23.3$, having used a value of the dust mass absorption coefficient $\kappa_{1500} = 1.26 \times 10^5 \text{ cm}^2 \text{ g}^{-1}$ appropriate for a MW-like extinction curve (Weingartner & Draine 2001, WD01).

By translating the observed $A_V = 0.31$ value into an optical depth, using $\tau_{1500} = 2.655(A_V/1.086)$, where the pre-factor accounts for the differential attenuation between 1500 \AA and the V-band for a MW curve, we find $\tau_{1500} = 0.76$, a value ≈ 30 times smaller than τ_{1500}^e .

Using the AFM to predict the star formation history of GS-z14-0, Ferrara (2024b) found that this galaxy has recently undergone a super-Eddington phase in which a powerful outflow has mini-quenched its star formation leaving it in the observed post-stardust phase. The outflow has ejected a significant fraction of the dust, metals and gas previously contained in r_e .

From the previous estimates we see that to decrease A_V to its observed value, the dust has to be re-configured by the outflow into a much more extended distribution of radius $r_d = (\tau_{1500}^e / \tau_{1500})^{1/2} r_e = 5.5 r_e$, which corresponds to $r_d \simeq 1.4$ kpc, for the fiducial ξ_d value.

Without the outflow hypothesis, to make the galaxy optically thin one should assume an extremely low dust content, corresponding to $\xi_d = 6.6 \times 10^{-5}$. For comparison, for galaxies in the REBELS sample (Bouwens et al. 2022) $\xi_d \approx 0.01$ (Ferrara et al. 2022; Dayal et al. 2022; Sommovigo et al. 2022). The results presented below explore both (and additional) possibilities showing that ALMA observations can clearly discriminate between these two alternative scenarios by detecting the FIR dust emission.

2.3. Dust temperature

Dust grains are heated by absorption of UV photons whose energy is re-emitted in the FIR. Depending on the assumed spatial distribution, grains can achieve different temperatures, thus affecting the emitted FIR flux. The latter is computed here at a rest frame wavelength of $88 \mu\text{m}$ since high- z ALMA observations are often tuned to detect [OIII] $88 \mu\text{m}$ line emission (Popping 2022; Bakx et al. 2022; Kaasinen et al. 2022; Fujimoto et al. 2023b; Kohandel et al. 2023)

The emitted radiation spectrum is classically modelled (e.g. Dayal et al. 2010; Hirashita et al. 2014) as a grey-body at mean dust temperature, \bar{T}_d , given by

$$\bar{T}_d = \left(\frac{L_{\text{abs}}}{\Theta M_d} \right)^{1/(4+\beta_d)}, \quad (1)$$

where

$$\Theta = \frac{8\pi \kappa_{88} k_B^{4+\beta_d}}{c^2 \nu_{88}^{\beta_d} h_P^{3+\beta_d}} \zeta(4+\beta_d) \Gamma(4+\beta_d), \quad (2)$$

and $L_{\text{abs}} = L_{\text{bol}}(1 - e^{-\tau_{1500}})$ is the fraction of the stellar UV radiation that is absorbed by dust. The galaxy bolometric luminosity is written as $L_{\text{bol}} = f_{\text{bol}} L_{1500}$, where the intrinsic galaxy luminosity at 1500 \AA (L_{1500}) is obtained from the inferred star formation rate (SFR), via a conversion factor, $\mathcal{K}_{1500} [L_\odot / M_\odot \text{ yr}^{-1}]$, whose value has been chosen so to match the one used by the ALMA REBELS survey (Bouwens et al. 2022): $\mathcal{K}_{1500} \equiv L_{1500} / \text{SFR} = 0.587 \times 10^{10}$. Following Fiore et al. (2023), we adopt $f_{\text{bol}} = 2$.

We take the mass absorption coefficient κ_{88} and β_d consistently with the adopted WD01 extinction curve $\kappa_{88} = 34.15 \text{ cm}^2 \text{ g}^{-1}$, and $\beta_d = 2.03$; ζ and Γ are the Zeta and Gamma functions, respectively; finally, ν_{88} is the frequency corresponding to wavelength $\lambda = 88 \mu\text{m}$. Other symbols have the usual meaning.

The temperature in eq. 1 is a mean (or ‘‘effective’’) physical dust temperature such that energy balance between dust absorbed and emitted photon energy is guaranteed. In general, though, radiative transfer effects produce a temperature distribution, with T_d decreasing away from the source. It is therefore necessary to include a correction factor which becomes important when the system becomes optically thick.

Ferrara et al. (2022, see their Appendix A) showed that the luminosity-weighted temperature, $\langle T_d \rangle_L$, of an absorbing dust slab depends on its total optical depth, and can be written as

$$\langle T_d \rangle_L = \bar{T}_d \frac{6}{7} \frac{1/b}{\tau_{1500}^{1/b}} \frac{(1 - e^{-7\tau_{1500}/b})}{(1 - e^{-\tau_{1500}})^{7/b}} \equiv \bar{T}_d f_L(\tau_{1500}), \quad (3)$$

where $b = 4 + \beta_d$. Applying eq. 3 results in temperatures that are generally higher⁴ than \bar{T}_d . To conserve energy M_d must be reduced by a factor $f_L^{-(4+\beta_d)}$. In the following we denote this reduced dust mass by $M'_d = f_L^{-(4+\beta_d)} M_d$.

⁴ We neglect self-heating by the dust, i.e. absorption of thermal IR radiation emitted by the grains, as it becomes important at high optical depth (Gordon et al. 2017), while the configurations of interest here have $A_V < 1$.

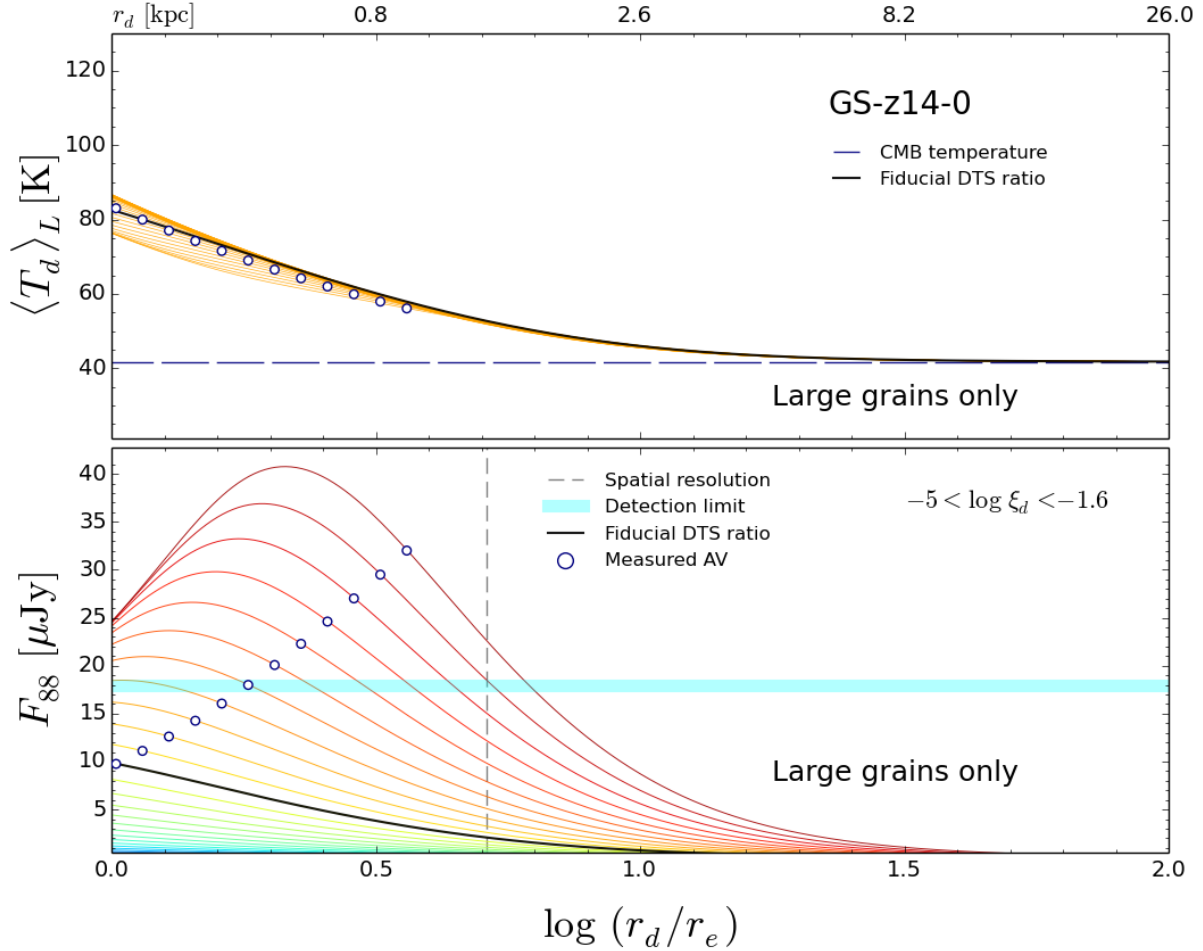


Figure 2. Same as Fig. 1, but assuming that the dust is constituted by large silicate grains with a log-normal distribution centered at $0.5 \mu\text{m}$, appropriate for grains freshly formed in SN ejecta.

2.4. Observed flux at $88\mu\text{m}$

From the previous results it is straightforward to compute the restframe $88 \mu\text{m}$ specific flux from a source at $z = z_s$ observed at wavelength $88(1 + z_s) \mu\text{m}$:

$$F_{88} = g(z_s) \kappa_{88} M'_d [B_{88}(T'_d) - B_{88}(T_{\text{CMB}})]; \quad (4)$$

B_λ is the black-body spectrum, and $T_{\text{CMB}}(z) = T_0(1 + z_s)$, with $T_0 = 2.7255 \text{ K}$ (Fixsen 2009) is the CMB temperature at redshift z_s . Equation 4 accounts for the fact that the CMB acts as a thermal bath for dust grains, setting a lower limit to their temperature. At $z_s = 14.32$ such minimum temperature corresponds to $T_{\text{CMB}} = 41.75 \text{ K}$. Finally, T'_d is the CMB-corrected dust

temperature⁵ following Da Cunha et al. (2013),

$$T'_d = \{ \langle T_d \rangle_L^{4+\beta_d} + T_0^{4+\beta_d} [(1+z)^{4+\beta_d} - 1] \}^{1/(4+\beta_d)}. \quad (5)$$

3. RESULTS

Fig. 1 summarises our predictions for the ALMA dust continuum emission from GS-z14-0. The top (bottom) panel shows the dependence of the luminosity-weighted dust temperature ($88 \mu\text{m}$ flux) for a spherical dust distribution of varying radius r_d , normalised to the observed effective stellar radius, r_e , of the galaxy. Each curve corresponds to a dust-to-stellar ratio, ξ_d , in the range $-5 < \log \xi_d < -1.6$ equally spaced in 0.1 logarithmic intervals with the black curve highlighting the fiducial case $\log \xi_d = -2.72$, or $\xi_d = 1/529$.

⁵ In the remainder of the paper we will always refer to dust temperature as the *CMB-corrected* one, i.e. T'_d in eq. 5.

The luminosity-weighted temperature trend can be understood with the help of eq. 3. Along each orange curve the dust mass $M_d = \xi_d M_\star$ is fixed. The most evident feature is the dust temperature decrease from 110 – 125 K at $r_d = r_e$ to the CMB temperature at the largest considered radii (17.5 kpc), where the dust becomes virtually undetectable. The temperature drop is due to the fact that as we consider more extended, and therefore more optically thin, dust distributions, the absorbed stellar radiation decreases, and the dust becomes colder. Note that if the dust had not been ejected from the galaxy, and therefore $r_d = r_e$, the dust-to-stellar ratio should be very small ($\log \xi_d = -4.2$) to yield the measured $A_V = 0.31$ (denoted by circles).

On top of this trend, at any given radius the curves differ by up to 10 – 20% as a result of variations of M_d from curve to curve, and due to the fact that for small radii, most curves (specifically, those with $\log \xi_d > -4.2$) correspond to optically thick regimes for which $\langle T_d \rangle_L$ is slightly larger (see eq. 3). This is easily seen by taking the optically thick limit $\tau_{1500} \rightarrow \infty$, in which $\langle T_d \rangle_L \propto \tau_{1500}^{1/(4+\beta_d)}$. For each curve the circles mark the radius at which the attenuation matches the observed value $A_V = 0.31$ (higher/lower A_V values to the left/right). For each value of ξ_d , the temperature indicated by the circle is then the “true” (i.e. predicted) one, within model assumptions.

The behavior of F_{88} in the optically thick regime can be understood as follows. From eq. 4, further neglecting CMB effects – which is appropriate given that dust is hot at small radii, it follows that $F_{88} \propto M' B_\nu(\langle T_d \rangle_L) \simeq M' \langle T_d \rangle_L$ in the Rayleigh-Jeans regime. We have already seen that $\langle T_d \rangle_L \propto \tau_{1500}^{1/(4+\beta_d)}$; also, $M'_d = f_L^{-(4+\beta_d)} M_d \propto \tau_{1500}^{-1}$. Hence, F_{88} decreases as $\tau_{1500}^{-(3+\beta_d)/(4+\beta_d)}$, which is exactly the trend shown in Fig. 1.

The corresponding 88 μm flux is shown in the bottom panel, where it is also compared with the expected 3σ continuum sensitivity (18 $\mu\text{Jy}/\text{beam}$) and spatial resolution (0.451”) of the ALMA DDT 2023.A.00037.S (PI: S. Schouws) observations of GS-z14-0. For each ξ_d value, the flux raises, reaches a peak (approximately where $\tau_{1500} \approx 1$), and decreases at large radii. The amplitude of the peak correlates with ξ_d . As the distribution becomes optically thick for small r_d/r_e values, the curves with larger ξ_d (or, equivalently, larger M_d) converge to a single line.

By looking at the circles ($A_V = 0.31$) we see that the fiducial model (black line, $\xi_d = 1/529$) predicts a 88 μm flux $F_{88}^{\text{fid}} = 14.9 \mu\text{Jy}$, essentially at the 3σ detection limit of the experiment, and a luminosity-weighted temperature of 72 K. As ξ_d is decreased, implying an efficient grain destruction by interstellar shocks, the signal be-

comes weaker and more difficult to detect. However, if the galaxy is dust-rich, at or above the level observed in some of the REBELS galaxies showing $\xi_d \approx 0.01$ (Ferrara et al. 2022; Dayal et al. 2022; Inami et al. 2022), the signal becomes detectable.

It is important to recall that the observed F_{88} measurement (or upper limit) should be interpreted along with the constraints provided by the observed A_V value. For example, suppose that – consistently with the fiducial model in Fig. 2 – F_{88} is measured to be 14.9 μJy (circle on black curve). Then, we would conclude that $\xi_d = 1/529$, and $\log(r_d^{\text{fid}}/r_e) \simeq 0.7$, or $r_d = 1.3$ kpc. If correct, ALMA observations should also show that the dust is spatially resolved, and more extended than the stellar component. The other, more compact solution for the same F_{88} , i.e. $\log(r_d/r_e) \simeq 0.4$, should be discarded because the galaxy would have an A_V much larger than observed.

A natural case to explore is the one in which the dust, in the absence of any ejective event, remains within r_e . In this scenario, the temperature would be significantly higher ($\simeq 100$ K) and the distribution optically thick. These two properties act as to dramatically suppress the flux: independently of ξ_d (unless extremely small), $F_{88} = 5.3 \mu\text{Jy}$. Detecting such a low flux would require very long integration times.

In conclusion, a positive detection would strongly support the hypothesis that dust produced by SNe associated with the observed stars in GS-z14-0 has been carried to larger galactocentric radii by outflows, making the galaxy bright and transparent to UV radiation. This conclusion highlights the key importance of ALMA deep observations of super-early galaxies.

3.1. Large grains

In addition to dust ejection or destruction by shocks, we need to consider a third possibility, i.e., that early dust is constituted by large, 0.1 – 1 μm size grains. The need is based on two facts: (a) theoretically, it is predicted that SN dust lacks small grains which are preferentially destroyed in the ejecta by the reverse shock (Nozawa et al. 2007; Asano et al. 2013; Hirashita & Aoyama 2019), (b) experimentally, the SED of galaxies in $z = 2 - 12$ *JWST*-detected galaxies show an increasingly flatter extinction curve towards high- z (Di Mascia et al. 2021; Markov et al. 2024). These two evidences are clearly connected as large grains of size a absorb light with wavelength $\lambda \ll a$ in a frequency-independent way. In this case, the absorption cross section should be equal to the geometric one, and the UV absorption coefficient $\kappa_{\text{UV}}^{\text{large}} \simeq 3/4 \delta_g a$, where $\delta_g = 2.95 \text{ g cm}^{-3}$ is the material density of silicate grains, i.e. those pref-

Table 1. Relevant properties of the selected super-early galaxies at $z > 10$

ID	redshift	A_V [mag]	SFR [$M_\odot \text{yr}^{-1}$]	$\log(M_*/M_\odot)$	r_e [pc]	F_{88}^{fid} [μJy]	F_{88}^{max} [μJy]	$\log(r_d^{\text{fid}}/r_e)$
GS-z14-0 ^a	14.32	$0.31^{+0.14}_{-0.17}$	22^{+6}_{-6}	$8.60^{+0.7}_{-0.2}$	260^{+2}_{-2}	14.9	40.1	0.73
GS-z14-1 ^a	13.90	$0.20^{+0.11}_{-0.07}$	$2^{+0.7}_{-0.4}$	$8.00^{+0.4}_{-0.4}$	< 160	2.0	3.8	0.70
UNCOVER-z12 ^b	12.39	$0.19^{+0.17}_{-0.10}$	$3.08^{+1.81}_{-0.68}$	$8.35^{+0.21}_{-0.16}$	426^{+40}_{-42}	4.4	8.5	0.47
GS-z11-0 ^c	11.58	$0.18^{+0.06}_{-0.06}$	$2.20^{+0.28}_{-0.22}$	$8.67^{+0.08}_{-0.13}$	77 [†]	5.2	7.8	1.38
GHZ2 ^d	12.34	$0.04^{+0.07}_{-0.03}$	$5.2^{+1.1}_{-0.6}$	$9.05^{+0.10}_{-0.25}$	105^{+9}_{-9}	3.4	4.0	1.76

NOTE—The measured values are taken from the following references: ^aCarniani et al. (2024); Robertson et al. (2023b), ^bWang et al. (2023); Fujimoto et al. (2023a); Atek et al. (2022), ^dCurtis-Lake et al. (2023); Robertson et al. (2023a), ^dCastellano et al. (2024); [†]Error not provided. The last three columns show the predictions of the model for the fiducial (maximum) 88 μm observed flux, and the fiducial dust-to-stellar radius ratio for which A_V matches the observed value, respectively.

entially produced by SNe. Note that if $a = 0.5 \mu\text{m}$, $\kappa_{\text{UV}}^{\text{large}} = 0.04\kappa_{\text{UV}}$.

These estimates are confirmed by detailed calculations performed by Ysard et al. (2019) that we use here. These authors compute the optical properties of 0.01 μm to 10 cm grains from effective medium and Mie theories. To this aim they assume a lognormal distribution of grain sizes centered at a given radius, a_0 , which we assume to be equal to 0.5 μm according to the previous discussion, and a fixed dispersion $\sigma = 0.7$. With these assumptions they indeed find $\kappa_{\text{UV}}^{\text{large}} \simeq 3/4\delta_g a = 5085 \text{ cm}^2\text{g}^{-1}$, and $\kappa_{88}^{\text{large}} = 15 \text{ cm}^2\text{g}^{-1}$.

Fig. 2 presents the temperature and expected flux if dust is composed by large $\simeq 0.5 \mu\text{m}$ grains. The temperature follows the same trend as in the standard case, but it is significantly colder, reaching at r_e values in the range 75–85 K. As a result, for any given ξ_d , the flux is smaller, e.g. $F_{88}^{\text{fid}} = 9.5 \mu\text{Jy}$, and shifted to smaller radii compared to the standard case. Also, the lower opacity of large grains allows the galaxy to become optically thin (as observed) for more compact distributions.

3.2. Other super-early galaxies

Our model can be used to make predictions on the FIR observability of other potentially detectable super-early galaxies. In addition to GS-z14-0, which has the largest A_V among $z > 10$ spectroscopically confirmed galaxies, we have selected the next three dustiest galaxies, GS-z14-1 ($A_V = 0.20$), UNCOVER-z12 (0.19), GS-z11-0 (0.18). We have also included GHZ2 in spite of its very low attenuation ($A_V = 0.04$, Castellano et al. 2024, but see Zavala et al. 2024 who find $A_V = 0.01 - 0.2$ depending of the SED fitter used) because of its very interesting spectrum showing many prominent emission lines.

The relevant properties (redshift, A_V , SFR, M_* , r_e) of the galaxies in the sample are reported in Tab. 1, along with the predicted value of the fiducial 88 μm flux,

and the radius r_d^{fid} where the attenuation becomes equal to the observed A_V value. Also shown is the maximum expected flux, F_{88}^{max} which we take from the curve with the maximum assumed value of $\log \xi_d = -1.6$.

For the galaxies in the sample the dust temperature and the FIR flux follow very similar trends with r_d/r_e as shown in Fig. 1 for GS-z14-0, albeit they quantitatively differ as a result of the different properties of the galaxy. From the Table, we see that the expected fiducial fluxes range from 2 μJy for the faintest galaxy (GS-z14-1) to 14.9 μJy for the brightest (and most distant) one, GS-z14-0; the latter therefore remains the most promising target to constrain the dust content of the very early galaxies. For GHZ2, if we instead assume the largest attenuation found by Zavala et al. (2024), $A_V = 0.2$, we find a larger fiducial and maximum flux, $F_{88}^{\text{fid}} = 11.2 \mu\text{Jy}$, and $F_{88}^{\text{max}} = 16.3 \mu\text{Jy}$, respectively.

Finally, notice that we did not considered the remarkable galaxy GN-z11 (Bunker et al. 2023) as it is not visible by ALMA due to its northern emisphere location. However, this galaxy has been observed by the Northern Extended Millimeter Array (NOEMA, Fudamoto et al. 2023). These observations, have put a 1σ upper limit of 13 $\mu\text{Jy}/\text{beam}$ at 160 μm . When applied to GN-z11, our model (fiducial case) predicts a maximum flux $F_{160}^{\text{max}} = 14.1 \mu\text{Jy}$. Although interesting, available NOEMA observations are unfortunately too shallow to detect the expected signal.

4. SUMMARY

To test one of the predictions of the ‘‘Attenuation-Free Model’’ (Ferrara et al. 2023; Ferrara 2024a), we have modelled the FIR dust continuum emission from the extended dust distribution produced by outflows around ‘‘blue monsters’’, i.e. luminous, blue, super-early ($z > 10$) galaxies. Given the observed properties of the galaxies (redshift, A_V , SFR, M_* , r_e), the expected

flux at 88 μm depends on the dust-to-stellar ratio, ξ_d , and extent of the dust distribution, r_d . A signal detection with ALMA would therefore constrain the amount of dust and its extent, thus representing a successful test that the attenuation-free conditions are produced by dust ejection by (likely, radiation-driven) outflows. We have discussed in detail GS-z14-0 ($z = 14.32$), and further applied the model to other 4 super-early galaxies. We find that:

- If the dust is in the galaxy ($r_d = r_e$) its temperature is 110 – 125 K. In this case, though, the dust-to stellar mass ratio must be very small ($\log \xi_d < -4.2$) not to exceed the measured $A_V = 0.31$. For $r_d > r_e$, $\langle T_d \rangle_L$ decreases asymptotically towards T_{CMB} (Fig. 1, top panel).
- The fiducial model ($\xi_d = 1/529$) predicts for GS-z14-0 an observed flux $F_{88}^{\text{fid}} = 14.9 \mu\text{Jy}$, and a dust extent $r_d \sim 1.4 \text{ kpc}$ (Fig. 1, bottom panel). For the largest value considered, $\log \xi_d = -1.6$, $F_{88}^{\text{max}} = 40.1 \mu\text{Jy}$. These values are smaller ($F_{88}^{\text{fid}} = 9.5 \mu\text{Jy}$) if the dust is predominantly made of large grains as those formed in SN ejecta (Fig. 2).
- Forthcoming ALMA observations, with an expected 3σ sensitivity of $18\mu\text{Jy}$, should come very close to constraining the fiducial predictions of the outflow-based attenuation-free model.

- Other super-early galaxies are predicted (Tab. 1) to be fainter at 88 μm , mostly because of their lower SFR compared to GS-z14-0 but also due to their lower A_V , with fiducial fluxes in the range $F_{88}^{\text{fid}} = 2 - 5.2 \mu\text{Jy}$.

We conclude by warning that albeit our model is built to catch the main features of the AFM, its simple incarnation cannot include potentially non-negligible effects that might quantitatively change our conclusions. For example, the present study does not account for self-heating of the dust by re-processed thermal photons, dust scattering and grain size distribution. The impact of these effects on the results presented here can only be ascertained via dedicated numerical radiative transfer simulations.

ACKNOWLEDGMENTS

We thank J. Zavala and M. Castellano for useful discussions, data and comments. This work is supported by the ERC Advanced Grant INTERSTELLAR H2020/740120, and in part by grant NSF PHY-2309135 to the Kavli Institute for Theoretical Physics (KITP). Plots in this paper produced with the MATPLOTLIB (Hunter 2007) package for PYTHON.

REFERENCES

- Arrabal Haro, P., Dickinson, M., Finkelstein, S. L., et al. 2023, arXiv e-prints, arXiv:2304.05378, doi: [10.48550/arXiv.2304.05378](https://doi.org/10.48550/arXiv.2304.05378)
- Asano, R. S., Takeuchi, T. T., Hirashita, H., & Inoue, A. K. 2013, *Earth, Planets, and Space*, 65, 213, doi: [10.5047/eps.2012.04.014](https://doi.org/10.5047/eps.2012.04.014)
- Atek, H., Shuntov, M., Furtak, L. J., et al. 2022, *Revealing Galaxy Candidates out to $z \sim 16$ with JWST Observations of the Lensing Cluster SMACS0723*, arXiv, doi: [10.48550/ARXIV.2207.12338](https://doi.org/10.48550/ARXIV.2207.12338)
- Bakx, T. J. L. C., Zavala, J. A., Mitsuhashi, I., et al. 2022, arXiv e-prints, arXiv:2208.13642, <https://arxiv.org/abs/2208.13642>
- Bouwens, R. J., Smit, R., Schouws, S., et al. 2022, *ApJ*, 931, 160, doi: [10.3847/1538-4357/ac5a4a](https://doi.org/10.3847/1538-4357/ac5a4a)
- Bunker, A. J., Saxena, A., Cameron, A. J., et al. 2023, arXiv e-prints, arXiv:2302.07256, doi: [10.48550/arXiv.2302.07256](https://doi.org/10.48550/arXiv.2302.07256)
- Calabro, A., Castellano, M., Zavala, J. A., et al. 2024, arXiv e-prints, arXiv:2403.12683, doi: [10.48550/arXiv.2403.12683](https://doi.org/10.48550/arXiv.2403.12683)
- Carniani, S., Hainline, K., D'Eugenio, F., et al. 2024, arXiv e-prints, arXiv:2405.18485, doi: [10.48550/arXiv.2405.18485](https://doi.org/10.48550/arXiv.2405.18485)
- Castellano, M., Napolitano, L., Fontana, A., et al. 2024, arXiv e-prints, arXiv:2403.10238, doi: [10.48550/arXiv.2403.10238](https://doi.org/10.48550/arXiv.2403.10238)
- Curti, M., D'Eugenio, F., Carniani, S., et al. 2022, *MNRAS*, doi: [10.1093/mnras/stac2737](https://doi.org/10.1093/mnras/stac2737)
- Curtis-Lake, E., Carniani, S., Cameron, A., et al. 2023, *Nature Astronomy*, doi: [10.1038/s41550-023-01918-w](https://doi.org/10.1038/s41550-023-01918-w)
- Da Cunha, E., Groves, B., Walter, F., et al. 2013, *The Astrophysical Journal*, 766, 13
- Dayal, P., Hirashita, H., & Ferrara, A. 2010, *MNRAS*, 403, 620, doi: [10.1111/j.1365-2966.2009.16164.x](https://doi.org/10.1111/j.1365-2966.2009.16164.x)
- Dayal, P., Ferrara, A., Sommovigo, L., et al. 2022, *MNRAS*, 512, 989, doi: [10.1093/mnras/stac537](https://doi.org/10.1093/mnras/stac537)

- Dekel, A., Sarkar, K. S., Birnboim, Y., Mandelker, N., & Li, Z. 2023, arXiv e-prints, arXiv:2303.04827, doi: [10.48550/arXiv.2303.04827](https://doi.org/10.48550/arXiv.2303.04827)
- Di Mascia, F., Gallerani, S., Behrens, C., et al. 2021, MNRAS, 503, 2349, doi: [10.1093/mnras/stab528](https://doi.org/10.1093/mnras/stab528)
- Ferrara, A. 2024a, A&A, 684, A207, doi: [10.1051/0004-6361/202348321](https://doi.org/10.1051/0004-6361/202348321)
- . 2024b, arXiv e-prints, arXiv:2405.20370, doi: [10.48550/arXiv.2405.20370](https://doi.org/10.48550/arXiv.2405.20370)
- Ferrara, A., Pallottini, A., & Dayal, P. 2023, MNRAS, 522, 3986, doi: [10.1093/mnras/stad1095](https://doi.org/10.1093/mnras/stad1095)
- Ferrara, A., Viti, S., & Ceccarelli, C. 2016, MNRAS, 463, L112, doi: [10.1093/mnrasl/slw165](https://doi.org/10.1093/mnrasl/slw165)
- Ferrara, A., Sommovigo, L., Dayal, P., et al. 2022, MNRAS, 512, 58, doi: [10.1093/mnras/stac460](https://doi.org/10.1093/mnras/stac460)
- Ferrarotti, A. S., & Gail, H. P. 2006, A&A, 447, 553, doi: [10.1051/0004-6361:20041198](https://doi.org/10.1051/0004-6361:20041198)
- Finkelstein, S. L., Leung, G. C. K., Bagley, M. B., et al. 2023, arXiv e-prints, arXiv:2311.04279, doi: [10.48550/arXiv.2311.04279](https://doi.org/10.48550/arXiv.2311.04279)
- Fiore, F., Ferrara, A., Bischetti, M., Feruglio, C., & Travascio, A. 2023, ApJL, 943, L27, doi: [10.3847/2041-8213/acb5f2](https://doi.org/10.3847/2041-8213/acb5f2)
- Fixsen, D. J. 2009, ApJ, 707, 916, doi: [10.1088/0004-637X/707/2/916](https://doi.org/10.1088/0004-637X/707/2/916)
- Fudamoto, Y., Oesch, P. A., Walter, F., et al. 2023, arXiv e-prints, arXiv:2309.02493, doi: [10.48550/arXiv.2309.02493](https://doi.org/10.48550/arXiv.2309.02493)
- Fujimoto, S., Wang, B., Weaver, J., et al. 2023a, arXiv e-prints, arXiv:2308.11609, doi: [10.48550/arXiv.2308.11609](https://doi.org/10.48550/arXiv.2308.11609)
- Fujimoto, S., Finkelstein, S. L., Burgarella, D., et al. 2023b, ApJ, 955, 130, doi: [10.3847/1538-4357/aceb67](https://doi.org/10.3847/1538-4357/aceb67)
- Gordon, K. D., Baes, M., Bianchi, S., et al. 2017, A&A, 603, A114, doi: [10.1051/0004-6361/201629976](https://doi.org/10.1051/0004-6361/201629976)
- Helton, J. M., Rieke, G. H., Alberts, S., et al. 2024, arXiv e-prints, arXiv:2405.18462, doi: [10.48550/arXiv.2405.18462](https://doi.org/10.48550/arXiv.2405.18462)
- Hirashita, H., & Aoyama, S. 2019, MNRAS, 482, 2555, doi: [10.1093/mnras/sty2838](https://doi.org/10.1093/mnras/sty2838)
- Hirashita, H., Ferrara, A., Dayal, P., & Ouchi, M. 2014, MNRAS, 443, 1704, doi: [10.1093/mnras/stu1290](https://doi.org/10.1093/mnras/stu1290)
- Hsiao, T. Y.-Y., Abdurro'uf, Coe, D., et al. 2023, arXiv e-prints, arXiv:2305.03042, doi: [10.48550/arXiv.2305.03042](https://doi.org/10.48550/arXiv.2305.03042)
- Hunter, J. D. 2007, Computing in Science and Engineering, 9, 90, doi: [10.1109/MCSE.2007.55](https://doi.org/10.1109/MCSE.2007.55)
- Inami, H., Algera, H., Schouws, S., et al. 2022, MNRAS, doi: [10.1093/mnras/stac1779](https://doi.org/10.1093/mnras/stac1779)
- Inayoshi, K., Harikane, Y., Inoue, A. K., Li, W., & Ho, L. C. 2022, ApJL, 938, L10, doi: [10.3847/2041-8213/ac9310](https://doi.org/10.3847/2041-8213/ac9310)
- Kaasinen, M., van Marrewijk, J., Popping, G., et al. 2022, arXiv e-prints, arXiv:2210.03754, <https://arxiv.org/abs/2210.03754>
- Kohandel, M., Ferrara, A., Pallottini, A., et al. 2023, MNRAS, 520, L16, doi: [10.1093/mnrasl/slac166](https://doi.org/10.1093/mnrasl/slac166)
- Leńniewska, A., & Michałowski, M. J. 2019, A&A, 624, L13, doi: [10.1051/0004-6361/201935149](https://doi.org/10.1051/0004-6361/201935149)
- Li, Z., Dekel, A., Sarkar, K. C., et al. 2023, arXiv e-prints, arXiv:2311.14662, doi: [10.48550/arXiv.2311.14662](https://doi.org/10.48550/arXiv.2311.14662)
- Liu, B., & Bromm, V. 2022, The Astrophysical Journal Letters, 937, L30, doi: [10.3847/2041-8213/ac927f](https://doi.org/10.3847/2041-8213/ac927f)
- Markov, V., Gallerani, S., Ferrara, A., et al. 2024, arXiv e-prints, arXiv:2402.05996, doi: [10.48550/arXiv.2402.05996](https://doi.org/10.48550/arXiv.2402.05996)
- Martínez-González, S., Wünsch, R., Silich, S., et al. 2019, ApJ, 887, 198, doi: [10.3847/1538-4357/ab571b](https://doi.org/10.3847/1538-4357/ab571b)
- Mason, C. A., Trenti, M., & Treu, T. 2023, MNRAS, 521, 497, doi: [10.1093/mnras/stad035](https://doi.org/10.1093/mnras/stad035)
- Matsuura, M., Dwek, E., Barlow, M. J., et al. 2015, ApJ, 800, 50, doi: [10.1088/0004-637X/800/1/50](https://doi.org/10.1088/0004-637X/800/1/50)
- Mirocha, J., & Furlanetto, S. R. 2023, MNRAS, 519, 843, doi: [10.1093/mnras/stac3578](https://doi.org/10.1093/mnras/stac3578)
- Naidu, R. P., Oesch, P. A., van Dokkum, P., et al. 2022, ApJL, 940, L14, doi: [10.3847/2041-8213/ac9b22](https://doi.org/10.3847/2041-8213/ac9b22)
- Niculescu-Duvaz, M., Barlow, M. J., Bevan, A., Milisavljevic, D., & Looze, I. D. 2021, The dust mass in Cassiopeia A from infrared and optical line flux differences. <https://arxiv.org/abs/2103.12705>
- Nozawa, T., Kozasa, T., Habe, A., et al. 2007, ApJ, 666, 955, doi: [10.1086/520621](https://doi.org/10.1086/520621)
- Pallottini, A., & Ferrara, A. 2023, arXiv e-prints, arXiv:2307.03219, doi: [10.48550/arXiv.2307.03219](https://doi.org/10.48550/arXiv.2307.03219)
- Planck Collaboration, Ade, P. A. R., Aghanim, N., et al. 2014, A&A, 571, A16, doi: [10.1051/0004-6361/201321591](https://doi.org/10.1051/0004-6361/201321591)
- Popping, G. 2022, arXiv e-prints, arXiv:2208.13072, <https://arxiv.org/abs/2208.13072>
- Priestley, F. D., De Looze, I., & Barlow, M. J. 2021, MNRAS, 502, 2438, doi: [10.1093/mnras/stab122](https://doi.org/10.1093/mnras/stab122)
- Rasmussen Cueto, E., Hutter, A., Dayal, P., et al. 2023, arXiv e-prints, arXiv:2312.12109, doi: [10.48550/arXiv.2312.12109](https://doi.org/10.48550/arXiv.2312.12109)
- Rho, J., Gomez, H. L., Boogert, A., et al. 2018, MNRAS, 479, 5101, doi: [10.1093/mnras/sty1713](https://doi.org/10.1093/mnras/sty1713)
- Robertson, B., Johnson, B. D., Tacchella, S., et al. 2023a, arXiv e-prints, arXiv:2312.10033, doi: [10.48550/arXiv.2312.10033](https://doi.org/10.48550/arXiv.2312.10033)

- . 2023b, arXiv e-prints, arXiv:2312.10033,
doi: [10.48550/arXiv.2312.10033](https://doi.org/10.48550/arXiv.2312.10033)
- Schneider, R., & Maiolino, R. 2024, *A&A Rv*, 32, 2,
doi: [10.1007/s00159-024-00151-2](https://doi.org/10.1007/s00159-024-00151-2)
- Sommovigo, L., Ferrara, A., Pallottini, A., et al. 2022,
MNRAS, 513, 3122, doi: [10.1093/mnras/stac302](https://doi.org/10.1093/mnras/stac302)
- Tacchella, S., Eisenstein, D. J., Hainline, K., et al. 2023,
arXiv e-prints, arXiv:2302.07234,
doi: [10.48550/arXiv.2302.07234](https://doi.org/10.48550/arXiv.2302.07234)
- Todini, P., & Ferrara, A. 2001, *MNRAS*, 325, 726,
doi: [10.1046/j.1365-8711.2001.04486.x](https://doi.org/10.1046/j.1365-8711.2001.04486.x)
- Valiante, R., Schneider, R., Bianchi, S., & Andersen, A. C.
2009, *MNRAS*, 397, 1661,
doi: [10.1111/j.1365-2966.2009.15076.x](https://doi.org/10.1111/j.1365-2966.2009.15076.x)
- Wang, B., Fujimoto, S., Labbé, I., et al. 2023, *The
Astrophysical Journal Letters*, 957, L34,
doi: [10.3847/2041-8213/acfe07](https://doi.org/10.3847/2041-8213/acfe07)
- Weingartner, J. C., & Draine, B. T. 2001, *ApJ*, 548, 296,
doi: [10.1086/318651](https://doi.org/10.1086/318651)
- Ysard, N., Koehler, M., Jimenez-Serra, I., Jones, A. P., &
Verstraete, L. 2019, *A&A*, 631, A88,
doi: [10.1051/0004-6361/201936089](https://doi.org/10.1051/0004-6361/201936089)
- Zavala, J. A., Castellano, M., Akins, H. B., et al. 2024,
arXiv e-prints, arXiv:2403.10491,
doi: [10.48550/arXiv.2403.10491](https://doi.org/10.48550/arXiv.2403.10491)
- Ziparo, F., Ferrara, A., Sommovigo, L., & Kohandel, M.
2023, *MNRAS*, 520, 2445, doi: [10.1093/mnras/stad125](https://doi.org/10.1093/mnras/stad125)